




Article

Kurarinone from *Sophora Flavescens* Roots Triggers ATF4 Activation and Cytostatic Effects Through PERK Phosphorylation

Sakiko Nishikawa ^{1,†}, Yuka Itoh ^{1,2,†}, Muneshige Tokugawa ¹, Yasumichi Inoue ^{1,3,*} , Ken-ichi Nakashima ⁴ , Yuka Hori ¹, Chiharu Miyajima ^{1,3}, Kou Yoshida ¹, Daisuke Morishita ¹, Nobumichi Ohoka ⁵, Makoto Inoue ⁴, Hajime Mizukami ^{6,‡}, Toshiaki Makino ⁶  and Hidetoshi Hayashi ^{1,3,*}

¹ Department of Cell Signaling, Graduate School of Pharmaceutical Sciences and Nagoya City University, Nagoya 467-8603, Japan

² Department of Biochemistry, Graduate School of Medicine, University of Yamanashi, Yamanashi 409-3898, Japan

³ Department of Innovative Therapeutic Sciences, Cooperative Major in Nanopharmaceutical Sciences, Graduate School of Pharmaceutical Sciences, Nagoya City University, Nagoya 467-8603, Japan

⁴ Laboratory of Medicinal Resources, School of Pharmacy, Aichi Gakuin University, Nagoya 464-8650, Japan

⁵ Division of Molecular Target and Gene Therapy Products, National Institute of Health Sciences, Kanagawa 210-9501, Japan

⁶ Department of Pharmacognosy, Graduate School of Pharmaceutical Sciences, Nagoya City University, Nagoya 467-8603, Japan

* Correspondence: yainoue@phar.nagoya-cu.ac.jp (Y.I.); hhayashi@phar.nagoya-cu.ac.jp (H.H.); Tel./Fax: +81-52-836-3484 (H.H.)

† These authors contributed equally to this work.

‡ Present address: The Kochi Prefectural Makino Botanical Garden, Kochi 781-8125, Japan.

Academic Editor: Tran Dang Xuan

Received: 8 August 2019; Accepted: 23 August 2019; Published: 27 August 2019



Abstract: In response to cellular stresses, activating transcriptional factor 4 (ATF4) regulates the expression of both stress-relieving genes and apoptosis-inducing genes, eliciting cell fate determination. Since pharmacological activation of ATF4 exerts potent anti-tumor effects, modulators of ATF4 activation may have potential in cancer therapy. We herein attempted to identify small molecules that activate ATF4. A cell-based screening to monitor *TRB3* promoter activation was performed using crude drugs used in traditional Japanese Kampo medicine. We found that an extract from *Sophora flavescens* roots exhibited potent *TRB3* promoter activation. The activity-guided fractionation revealed that kurarinone was identified as the active ingredient. Intriguingly, ATF4 activation in response to kurarinone required PKR-like endoplasmic reticulum kinase (PERK). Moreover, kurarinone induced the cyclin-dependent kinase inhibitor p21 as well as cytostasis in cancer cells. Importantly, the cytostatic effect of kurarinone was reduced by pharmacological inhibition of PERK. These results indicate that kurarinone triggers ATF4 activation through PERK and exerts cytostatic effects on cancer cells. Taken together, our results suggest that modulation of the PERK-ATF4 pathway with kurarinone has potential as a cancer treatment.

Keywords: ATF4; cancer; ISR; kurarinone; PERK; *Sophora flavescens*; *TRB3*

1. Introduction

The integrated stress response (ISR) is a fine-tuning signaling pathway present in eukaryotic cells that is activated by cells to adapt to a multitude of stresses, including endoplasmic reticulum (ER) stress,

glucose deprivation, amino acid deprivation, and hypoxia [1]. In the process of carcinogenesis, the ISR can be triggered by the activation of oncogenes or loss of function in tumor suppressor genes [2,3]. The ISR is initiated by the activation of eukaryotic initiation factor 2 α (eIF2 α) kinases. There are four members in mammals: double-stranded RNA-dependent protein kinase (PKR), PKR-like ER kinase (PERK), eIF2 α kinases heme-regulated inhibitor (HRI), and general control nonderepressible 2 (GCN2) [4]. Once activated, these eIF2 α kinases phosphorylate eIF2 α , which results in a global decrease in translation. Paradoxically, while the translation of most mRNAs is repressed, several mRNAs are able to bypass this translation block, such as activating transcription factor 4 (ATF4) mRNA, which regulates the transcription of various genes involved in the stress response [5].

ATF4 acts as a master regulator of cellular responses to stress [6]. ATF4 regulates the expression of a broad range of adaptive genes that help cells to withstand periods of stress; however, under persistent stress conditions, cell death pathways are activated. ATF4 induces the expression of proapoptotic effectors, such as C/EBP homologous protein (CHOP), p53 up-regulated modulator of apoptosis (PUMA/BBC3), and phorbol-12-myristate-13-acetate-induced protein 1 (PMAIP1/NOXA). ATF4 is often overexpressed in cancer cells and promotes cell proliferation, survival, and drug resistance [6–8]. In contrast, ATF4 activation has been shown to induce tumor cell death under stress conditions [9–11]. Since pharmacological activators of the UPR, such as bortezomib, exert potent anti-tumor effects, modulators of ATF4 activation have potential in the treatment of cancer.

Many medicines currently used have many compounds that were originally found in natural organisms. Furthermore, those compounds were developed into more effective and safe synthetic compounds by the addition of various modifications to their molecular structures based on natural chemical structures and the useful pharmacological effects of chemical constituents. Therefore, research to find natural products with new chemical structures and effective biological activities is very important for drug discovery research. We herein attempted to identify low molecular weight compounds that activate ATF4. A cell-based screening to monitor *TRB3* promoter activation, which is a downstream of ATF4 activation, was performed using crude drugs used in traditional Japanese Kampo medicine. Among many drugs, an extract from *Sophora flavescens* roots exhibited potent *TRB3* promoter activation, and kurarinone was identified as their active ingredient. Mechanistically, ATF4 activation in response to kurarinone required PERK. In addition, kurarinone induced the cyclin-dependent kinase (CDK) inhibitor p21 as well as cytostasis in cancer cells. Intriguingly, the cytostatic effect of kurarinone was reduced by pharmacological inhibition of PERK. These results suggest that modulation of the PERK-ATF4 pathway with kurarinone has potential in the treatment of cancer.

2. Results

2.1. Extract of *S. flavescens* Roots Induced ATF4 Activation

We previously reported that ATF4 activated the transcriptional activation of *TRB3* in response to a variety of stresses, including ER stress [12]. The *TRB3* promoter contains three tandem 33 base pair repeats and each contains a composite ATF4/CHOP site (ER stress response sequence, Figure 1A) [13]. To identify small molecules that modulate ATF4 activation, we established a HEK293 cell line that stably expresses a human *TRB3* promoter (P1-Luc, Figure 1A). This cell line was confirmed by demonstrating that luciferase activity was induced by the known ER stressor TM (Figure 1B). Subsequently, we screened a library consisting of 119 crude drug extracts that are used in Kampo medicine. We found that the extracts of *S. flavescens* roots and *Notopterygium incisum* roots showed a strong increase in *TRB3* promoter activity (Figure 1B and data not shown). Unfortunately, it has already been shown that faltarindiol contained in the roots of *N. incisum* activates ER stress response [14]. Therefore, we chose *S. flavescens* roots for further investigation.

Although the extract for screening was extracted with methanol (MeOH) alone to evaluate a variety of crude drugs, we changed the extraction solvent to efficiently purify the active ingredient. The dried roots were extracted with acetone to prepare the acetone extract, and then the residue was

extracted with MeOH to prepare the MeOH extract. A comparison of these two extracts revealed that *TRB3* promoter activity was markedly induced after exposure to the acetone extract but not the MeOH extract (data not shown). Furthermore, the weight of the acetone extract was much less than that of the methanol extract, suggesting that extraction with acetone would concentrate the active ingredient more. Therefore, the acetone extract was used as the starting material for activity-guided fractionation. The results of activity-guided fractionation of the acetone extract and the isolation of constituents are shown in Figure S1A. Fraction 3, which had the ability to induce ATF4 activation (Figure S1B), was further purified by preparative TLC to obtain the active compound. The compound was identified as kurarinone (Figure 1C) based on EIMS (m/z 438.52, calcd for $C_{26}H_{30}O_6^+$, 438.513) and 1H and ^{13}C -NMR spectroscopic analyses (Figure S2) [15].

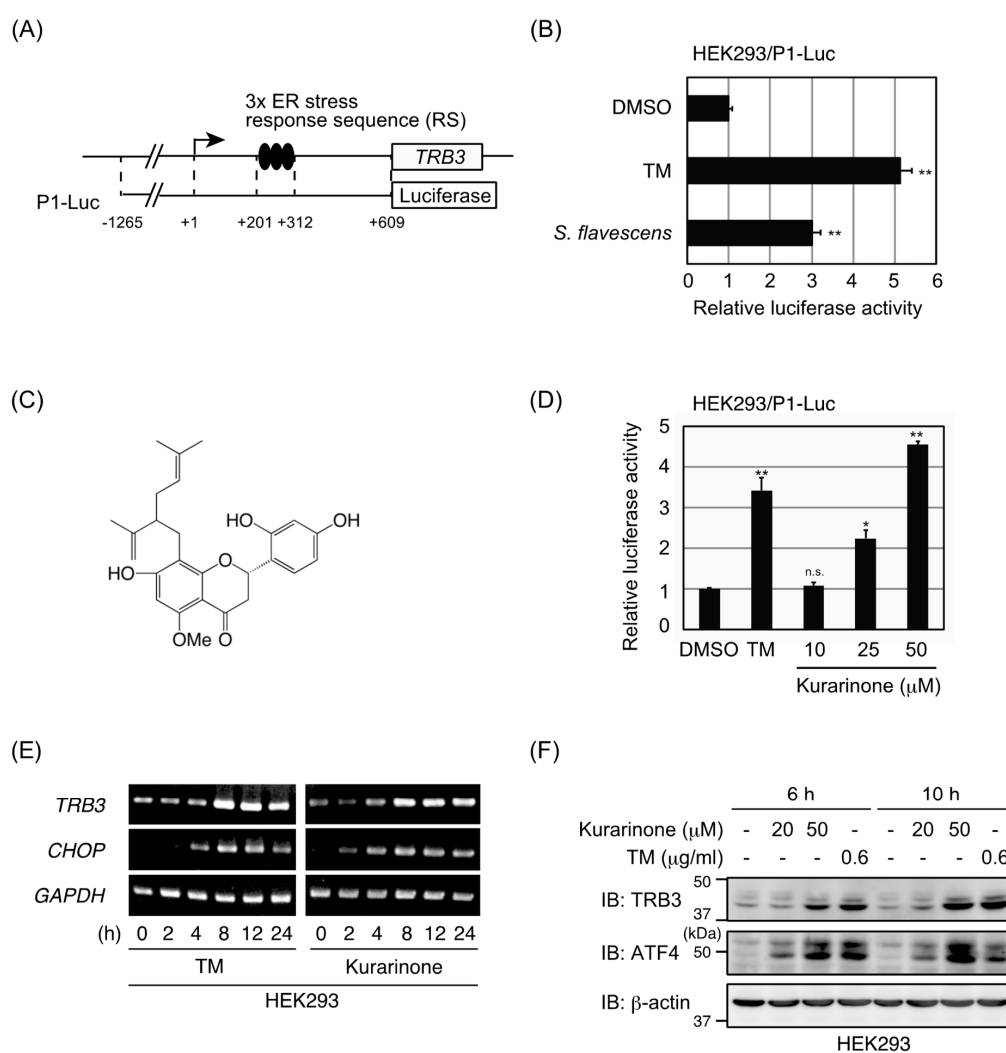
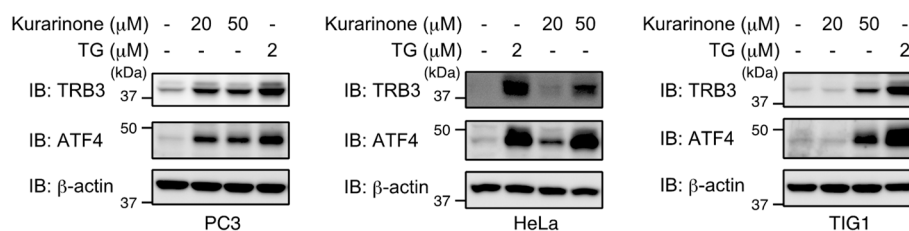


Figure 1. Extract of *Sophora flavescens* roots induced activating transcriptional factor 4 (ATF4) activation. (A) A schematic diagram of the human *TRB3* promoter plasmid. (B) HEK293/P1-Luc reporter cells were incubated with 2 µg/mL of tunicamycin (TM) or 100 µg/mL of the extract (ex.) of *S. flavescens* roots. After 24 h, luciferase activities were measured. Data represent the mean fold activation ± S.D. (n = 3). (C) Structure of kurarinone. (D) HEK293/P1-Luc reporter cells were incubated with 0.6 µg/mL of TM or the indicated doses of kurarinone. After 24 h, luciferase activities were measured as in (A). Data represent the mean fold activation ± S.D. (n = 3). (E) HEK293 cells were treated with 0.6 µg/mL of TM or 50 µM of kurarinone for the indicated times. The expression level of each gene was assessed by semiquantitative PCR. (F) HEK293 cells were incubated with the indicated doses of TM or kurarinone for the indicated periods. The level of the indicated proteins was determined by immunoblotting. Significant differences are indicated as ** $p < 0.01$. * $p < 0.05$. n.s.: not significant.

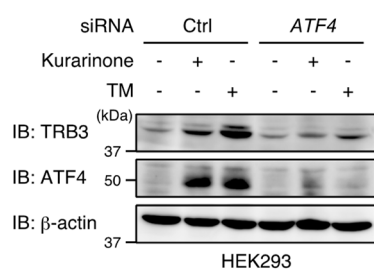
2.2. Kurarinone Induces TRB3 Expression in an ATF4-Dependent Manner

To demonstrate the effects of kurarinone on *TRB3* promoter activity, we performed a reporter assay on HEK293/P1-Luc reporter cells. As shown in Figure 1D, the kurarinone treatment upregulated the promoter activity of *TRB3* in a dose-dependent manner. Kurarinone also up-regulated the expression of *TRB3* and *CHOP* mRNAs as well as that of the TRB3 and ATF4 proteins in HEK293 cells (Figure 1E,F). The induction of TRB3 and ATF4 expression was also observed in PC3 cells (human prostate cancer), HeLa cells (human cervical cancer), and TIG1 cells (normal human diploid fibroblasts) (Figure 2A). To investigate whether ATF4 is required for the upregulation of TRB3 after exposure to kurarinone, ATF4 expression in HEK293 cells was suppressed by siRNA. As shown in Figure 2B, the knockdown of ATF4 inhibited the induction of the TRB3 protein upon the kurarinone treatment. Similar results were obtained using PC3 and HeLa cells (Figure 2C). These results indicate that ATF4 is responsible for the up-regulation of TRB3 by kurarinone.

(A)



(B)



(C)

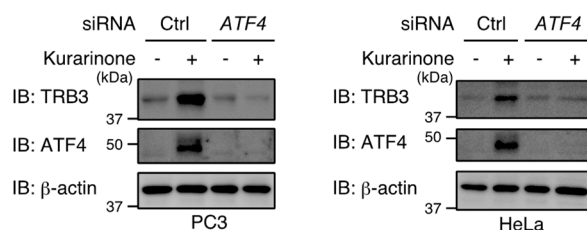


Figure 2. Kurarinone induces *TRB3* expression in an ATF4-dependent manner. **(A)** PC3 cells, HeLa cells, and TIG1 cells were treated with the indicated doses of thapsigargin (TG) or kurarinone for 6 h. Cell lysates were immunoblotted with the indicated antibodies. **(B)** HEK293 cells were transiently transfected with the indicated siRNAs. After 48 h, cells were treated with 0.6 μ g/mL of TM or 50 μ M of kurarinone for 6 h. Cell lysates were immunoblotted with the indicated antibodies as in **(A)**. **(C)** PC3 and HeLa cells were transiently transfected with the indicated siRNAs. After 48 h, cells were treated with 50 μ M of kurarinone for 6 h. Cell lysates were immunoblotted with the indicated antibodies as in **(A)**. Ctrl, control.

2.3. Kurarinone Triggers ATF4 Activation through the PERK-eIF2 α Pathway

Since ATF4 is the downstream effector of the ISR, we examined the effects of kurarinone on the initiation of the ISR. A band corresponding to PERK shifted when various cells were incubated with kurarinone (Figure 3A). Since the band was not shifted in the presence of GSK2656157, a catalytic inhibitor of PERK [16], kurarinone appears to have induced PERK phosphorylation (Figure 3B). The induction of ATF4 and TRB3 by kurarinone was also inhibited by GSK2656157 in PC3 cells. The knockdown of PERK also suppressed the induction of ATF4 and TRB3 upon the kurarinone treatment (Figure 3C). These results indicate that kurarinone activates ATF4 through the activation of PERK.

As described above, phosphorylation of eIF2 α leads to global translational repression while simultaneously stimulating several mRNAs, including ATF4. A small-molecule ISR inhibitor (ISRIB) was characterized that rescues translation in the presence of phosphorylated-eIF2 α by promoting the assembly of more active eIF2B [17,18]. As shown in Figure 3D, the pretreatment of ISRIB suppressed the induction of TRB3 and ATF4 after exposure to kurarinone, indicating that kurarinone activates ATF4 through the PERK-eIF2 α pathway. Of note, ISRIB did not suppress, but rather enhanced, the phosphorylation of PERK induced by kurarinone. Although GCN2 or PKR phosphorylate eIF2 α in response to various stresses, the treatment with kurarinone failed to induce the phosphorylation of these kinases (Figure 3E).

PERK represents one arm of the UPR, working in conjunction with two other ER-resident membrane proteins, activating transcription factor 6 (ATF6) and inositol-requiring enzyme 1 (IRE1) [1,19,20]. However, we found that kurarinone activated PERK without apparent activation of ATF6 or IRE1. While the treatment with TG induced discriminative target genes expression downstream of the three proteins, kurarinone only induced *TRB3* and *CHOP* mRNAs (downstream of PERK/ATF4) (Figure 3F). Collectively, these results indicate that kurarinone triggers ATF4 activation through the PERK-eIF2 α pathway.

2.4. Kurarinone Exerts Cytostatic Effects on Cancer Cells

Kurarinone has been reported to exhibit antitumor activity toward several cancer cells [21,22]. In the present study, it suppressed the proliferation of PC3 cells in a dose-dependent manner (Figure 4A). On the other hand, kurarinone exerted weak toxic effects on normal human diploid fibroblast TIG3 cells (Figure 4A). The selectivity index (SI) [23] of kurarinone between TIG3 cells and PC3 cells was more than 2.02. Thus, it was considered that antiproliferative activity of kurarinone is highly selective for cancer cells. The treatment with kurarinone resulted in less cell death but inhibited G₁ to S phase progression in PC3 cells (Figure 4B,C). We previously reported that the CDK inhibitor *p21* is a target gene of ATF4 and causes cell cycle arrest after ER stress [24]. Since the induction of *p21* causes G₁ arrest, we investigated whether the treatment with kurarinone upregulated *p21* protein expression in PC3 cells. As shown in Figure 4D, kurarinone significantly induced *p21* protein expression. Furthermore, the kurarinone treatment reduced the expression of cyclin D1 and cyclin A. These results suggest that *p21* upregulated by the PERK-ATF4 pathway contributes to the suppression of PC3 cell proliferation. We also examined whether the cytostatic effects of kurarinone were restored by inhibiting the activity of PERK. The treatment with GSK2656157 significantly recovered the growth arrest induced by kurarinone in PC3 cells (Figure 4E). Collectively, these results indicate that kurarinone triggers ATF4 activation through PERK-eIF2 α signaling and exerts cytostatic effects on cancer cells.

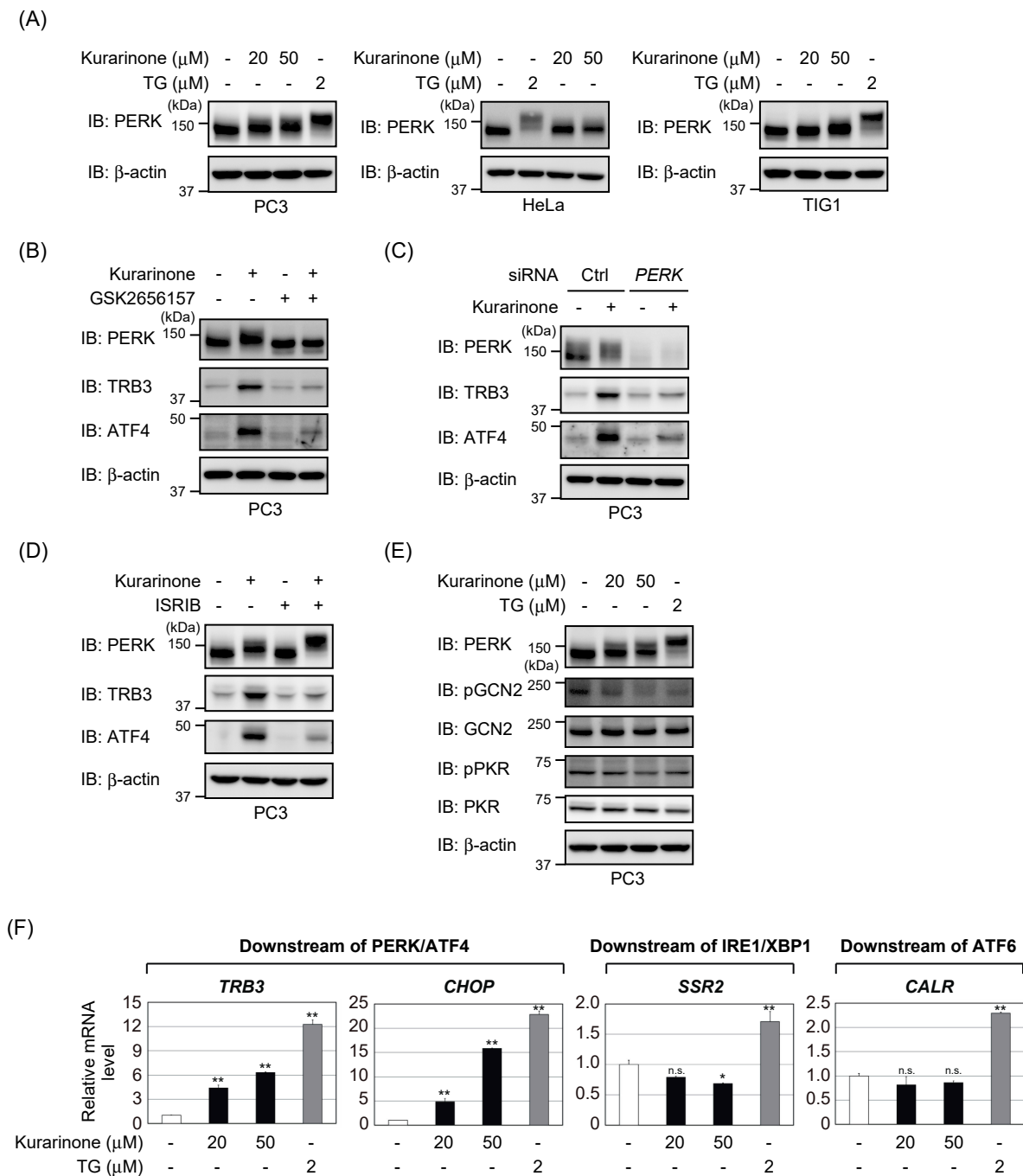


Figure 3. Kurarinone triggers ATF4 activation through the PERK-eIF2 α pathway. (A) PC3 cells, HeLa cells, and TIG1 cells were incubated with the indicated doses of thapsigargin (TG) or kurarinone for 6 h. The level of the indicated proteins was determined by immunoblotting. (B) PC3 cells were pretreated with 1 μM of GSK2656157 for 1 h and then incubated with 50 μM of kurarinone for 6 h. The level of the indicated proteins was determined by immunoblotting as in (A). (C) PC3 cells were transiently transfected with the indicated siRNAs. After 48 h of transfection, cells were incubated with 50 μM of kurarinone for 6 h. The level of the indicated proteins was determined by immunoblotting as in (A). Ctrl, control. (D) PC3 cells were pretreated with 0.5 μM of ISRIB for 1 h and then incubated with 50 μM of kurarinone for 6 h. Cell lysates were immunoblotted with the indicated antibodies as in (A). (E) PC3 cells were treated with the indicated doses of TG or kurarinone for 6 h. The level of the indicated proteins was determined by immunoblotting as in (A). (F) PC3 cells were incubated with the indicated doses of TG or kurarinone for 6 h. The expression level of each gene was assessed by quantitative PCR. Results represent the mean \pm S.D. ($n = 3$). Significant differences are indicated as ** $p < 0.01$. * $p < 0.05$. n.s.: not significant.

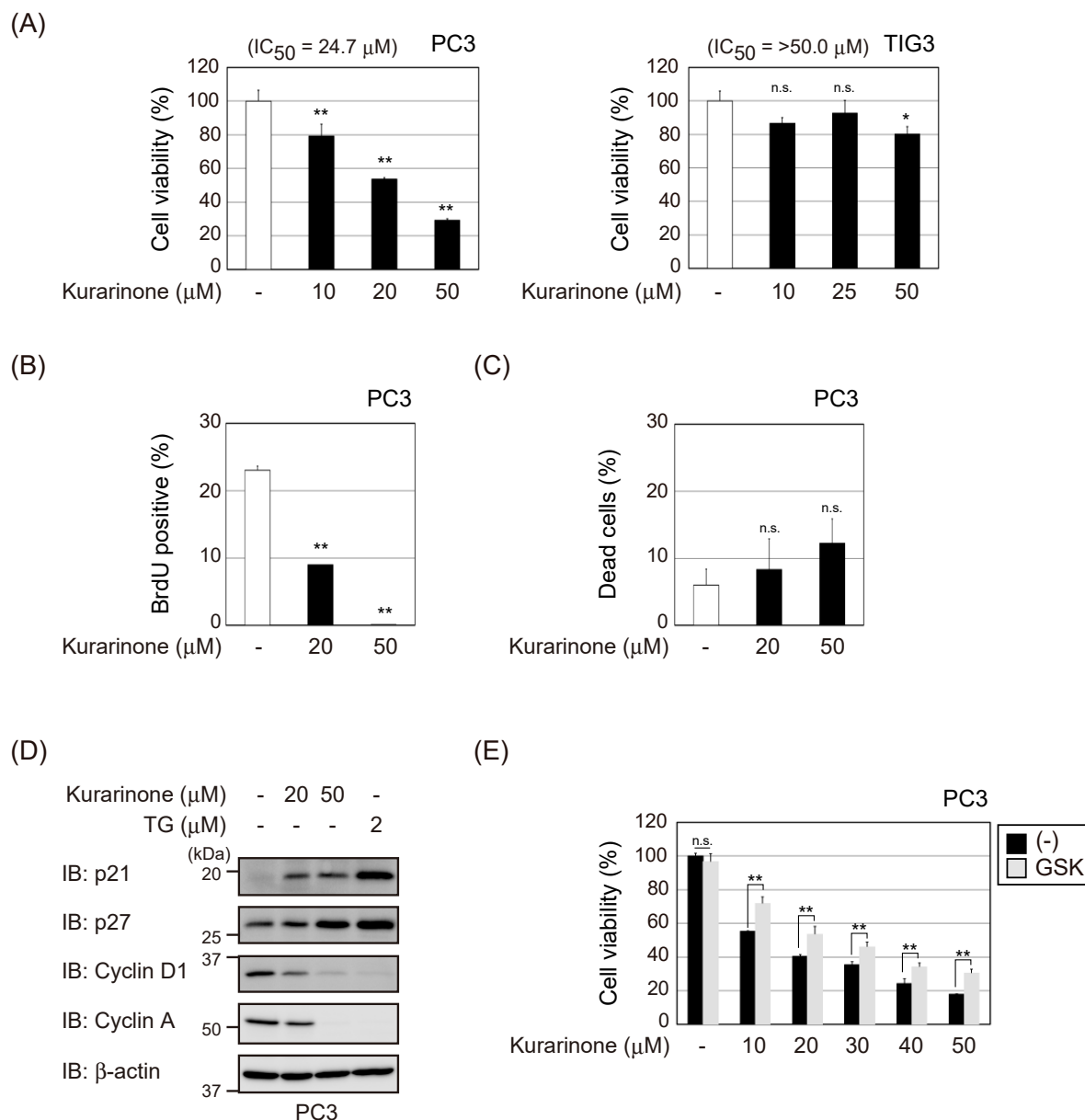


Figure 4. Kurarinone exerts cytostatic effects on cancer cells. (A) PC3 and TIG3 cells were incubated with the indicated doses of kurarinone for 48 h. Cell viability was determined by WST-8 assay. Results represent the mean \pm S.D. ($n = 3$). (B) PC3 cells were incubated with the indicated doses of kurarinone for 48 h. Cells were labeled with 10 μM of BrdU for 1 h and analyzed by fluorescence-activated cell sorting. The average percentage of BrdU-positive cells is shown. Results represent the mean \pm S.D. ($n = 3$). (C) PC3 cells were exposed to the indicated doses of kurarinone for 48 h. The percentage of dead cells was measured by trypan blue staining. Results were shown as the mean \pm S.D. ($n = 3$). (D) PC3 cells were incubated with the indicated doses of TG or kurarinone for 6 h. Cell lysates were immunoblotted with the indicated antibodies. (E) PC3 and TIG3 cells were exposed to the indicated doses of kurarinone with or without 1 μM of GSK2656157 (GSK) for 48 h. Cell viability was determined by WST-8 assay as in (A). Results represent the mean \pm S.D. ($n = 3$). Significant differences are indicated as ** $p < 0.01$. * $p < 0.05$. n.s.: not significant.

3. Discussion

In this paper, we demonstrated that kurarinone obtained from the roots of *S. flavescens* activated ATF4. Kurarinone activated PERK located upstream of eIF2 α and upregulated the expression of TRB3 and CHOP, which are target genes of the PERK-ATF4 pathway. Moreover, kurarinone induced

the CDK inhibitor p21 expression as well as cytostasis in cancer cells. The PERK-ATF4 pathway is recognized as a pathway related to cell cycle arrest and apoptosis in sensors that sense ER stress. Therefore, the development of drug discovery compounds that target the PERK-ATF4 pathway is underway [25–27]. Hence, modulation of the PERK-ATF4 pathway with kurarinone has potential as a therapeutic agent for drug discovery, particularly in the treatment of cancer.

S. flavescens roots, also known as “Kushen” in Chinese and “Kujin” in Japanese, have traditionally been mainly used in combination with other crude drugs in prescriptions to treat fever, dysentery, hematochezia, jaundice, oliguria, vulvar swelling, asthma, eczema, inflammatory disorders, ulcers, and diseases associated with skin burns [28]. Kurarinone, which is a lavandulyl flavanone, was previously reported to be abundant in *S. flavescens* roots [15,29]. Kurarinone possess numerous pharmacological activities, such as anti-inflammatory [30], anti-microbial [29], and cytotoxic activities against several cancer cells [21,22]. It has also been shown to inhibit the activity of NF- κ B [31] and promote TRAIL-induced apoptosis [32]. Previous studies reported that it activated the large-conductance calcium-activated potassium channel and has potential as a therapeutic drug for the treatment of diseases such as overactive bladder syndrome [33,34]. The present results indicate that kurarinone induces the phosphorylation of PERK; however, it failed to activate the IRE1 or ATF6 pathway. The mechanism of activation of PERK by kurarinone needs to be examined in more detail in future studies. In addition, it is necessary to evaluate the physicochemical and absorption, distribution, metabolism and excretion (ADME) properties of kurarinone. Although there are few reports on such properties of kurarinone, it has been reported that kurarinone showed hepatotoxicity [35]. Therefore, it is considered important to create a compound that exhibits anti-cancer activity while eliminating the hepatotoxicity of kurarinone.

In solid cancer, hypoxia and glucose deprivation occur due to the rapid growth of cancer cells and hypoplasia of blood vessels, and an environment with the constitutive activation of UPR is generated [36]. Most cancer cells are necrotic and ultimately die. However, some cancer cells survive and proliferate, thereby avoiding cell death even under this stress. These cancer cells constitutively active UPR and become more resistant to many anti-cancer agents. Therefore, an approach that controls the UPR of cancer cells in the cancer microenvironment is attracting attention as a new cancer therapy. By activating ATF4, research on compounds aimed at killing cancer cells is now being vigorously conducted. The proteasome inhibitor bortezomib triggers ER stress, activates ATF4, and induces cell death. Bortezomib has been reported to exhibit strong cytotoxic activity, particularly against mantle cell lymphoma, which is B-cell malignant lymphoma [37]. Furthermore, ONC201 is a compound currently undergoing clinical trials, and induces the phosphorylation of eIF2 α via PKR and HRI to express ATF4 and promote cell death [38,39]. Drug discovery aimed at promoting cancer cells to apoptosis through the induction of ATF4 is also underway.

In conclusion, kurarinone is expected to be a lead compound for new drugs that activate ATF4. Moreover, it may lead to the development of an effective therapeutics for the above-described intractable cancer. Further research is needed to elucidate the precise mode of action of kurarinone underlying the activation of the PERK-ATF4 pathway.

4. Materials and Methods

4.1. Cell Lines, Plasmids, and RNA Interference

PC3 cells were cultured in Roswell Park Memorial Institute 1640 medium (Sigma, St. Louis, MO, USA) containing 10% fetal bovine serum (FBS) (Sigma), 100 U/mL of penicillin G, and 100 μ g/mL of streptomycin [40]. HEK293, HeLa, TIG1, and TIG3 cells were maintained in Dulbecco’s modified Eagle’s medium (Sigma) supplemented with 4.5 g/L glucose, 10% FBS and penicillin/streptomycin [12,24].

TRB3 promoter P1-Luc (–1265 to +609) was constructed by ligating the human *TRB3* proximal promoter region [12] with pGL4.14 (Promega, Madison, WI, USA). HEK293 cells were transfected using the calcium phosphate method and selected with 100 μ g/mL hygromycin.

Regarding short interfering RNA (siRNA) transfection, siRNAs were transfected using Lipofectamine RNAiMAX reagent (Invitrogen, Carlsbad, CA, USA) according to the manufacturer's instructions. The siRNA oligo targeting human *ATF4* mRNA has been previously described [12]. Human *PERK* siRNA (sense: 5'-CACAAACUGUAUAACGGUU-3') was obtained from Sigma. Stealth RNAi™ siRNA Negative Control Med GC Duplex was purchased from Invitrogen.

4.2. RNA Extraction, Reverse Transcription, and PCR

The RNA extraction was carried out as previously described [41]. The cDNA was synthesized using the PrimeScript first-strand cDNA Synthesis Kit (TaKaRa Bio Inc., Shiga, Japan) [42]. Quantitative PCR was carried out as previously described [42]. Primers used for qPCR were as follows: human *TRB3*, 5'-TGACAACACTTTTCCATGACCATAG-3' (forward) and 5'-GGAGGCCGACACTGGTACAA-3' (reverse) [43]; human *CHOP*, 5'-GGTATGAGGACCTGCAAGAGGT-3' (forward) and 5'-CTTGTGACCTCTGCTGGTTCTG-3' (reverse) [44]; human β -actin, 5'-TGGCACCAGCACAATGAA-3' (forward) and 5'-CTAAGTCATAGTCCGCCTAGAAGCA-3' (reverse) [42]; human *SSR2*, 5'-TTCACCTCGGCAACAATTACT-3' (forward) and 5'-GGTGCCTGGTAGAGCCAAT-3' (reverse); human *CALR*, 5'-TGGCGTGCTGGGCCTGGACCTCTGG-3' (forward) and 5'-AAATGCACCATTCCTGAGA-3' (reverse) [45]. Values were normalized by β -actin. Semi-qPCR was carried out as previously described [46]. Primers used for semi-qPCR were as follows: human *TRB3*, 5'-TGCCCTACAGGCACTGAGTA-3' (forward) and 5'-GTCCGAGTGAAAAGGCGTA-3' (reverse) [47]; human *CHOP*, 5'-GCGTCTAGAATGGCAGCTGAGTCATTGCC-3' (forward) and 5'-GCGTCTAGATCATGCTTGGTGCAGATTC-3' (reverse) [12]; human *GAPDH*, 5'-TGAAGGTCGGAGTCAACGGATTTGGT-3' (forward) and 5'-CATGTGGGCCATGAGTCCACCAC-3' (reverse) [41].

4.3. Immunochemical Methods and Antibodies

Immunoblotting was carried out as previously described [48]. Commercially available antibodies used were as follows: anti-p21 (sc-6246; Santa Cruz Biotechnology, Santa Cruz, CA, USA), anti-p27 (610241; BD Biosciences, Franklin Lakes, NJ, USA), anti-cyclin A (611268; BD Biosciences), anti-cyclin D1 (556470; BD Biosciences), anti-ATF4 (11815; Cell Signaling Technology, Beverly, MA, USA), anti-PERK (5683; Cell Signaling Technology), anti-GCN2 (3302; Cell Signaling Technology), anti-TRB3 (ab75846; Abcam, Cambridge, UK), anti-phospho-GCN2 (T899) (ab75836; Abcam), anti-phospho-PKR (T451) (07-886; Sigma) anti- β -actin (A5441; Sigma), and anti-PKR (MAB1980; R&D Systems, Minneapolis, MN, USA).

4.4. Luciferase Assay

The luciferase reporter assay was carried out as previously described [41].

4.5. Cell Viability Assay and Cell Death Assay

Cell viability was determined using a cell counting kit-8 according to the manufacturer's protocol (Dojindo, Kumamoto, Japan). Cells were seeded at a density of 5×10^3 cells per well on a 96-well plate. After 24 h, cells were incubated with kurarinone for 48 h. The WST-8 solution was added and cells were incubated at 37 °C for 3 h in a humidified atmosphere of 5% CO₂. Absorbance of the medium was measured at the wavelength of 450 nm [24]. Regarding the quantification of cell death, cells were stained with trypan blue followed by counting with a hemocytometer under microscope. Stained cells were regarded as dead cells.

4.6. BrdU Incorporation Assay

Cells were treated with 10 μ M 5-bromo-2'-deoxyuridine (BrdU) at 37 °C for 1 h. BrdU-incorporated cells (S phase) were analyzed with the FITC BrdU Flow kit (BD Biosciences) according to the manufacturer's protocol. Cells were analyzed using a FACSVerse™ flow cytometer (BD Biosciences).

4.7. Preparation of Crude Drug Extracts

The extraction solvent selected for the present study was methanol (MeOH), and 119 crude drugs, which have been used in Japanese traditional Kampo medicine [49], were purchased from Tsumura (Tokyo, Japan). Cut crude drugs (5 g) were stirred in 50 mL of MeOH at room temperature for 24 h and were then filtered using filter paper. This process was repeated three times, and the extracts obtained were pooled. These pooled filtrates were concentrated in vacuo, the residue was dissolved in H₂O, and the aqueous solution was lyophilized. The lyophilisate was redissolved in dimethyl sulfoxide (DMSO) and stored at −20 °C until used. Screening was performed with crude drug extracts at 100 μ g/mL.

4.8. Extraction and Isolation of Kurarinone from *S. Flavescens* Roots

The dried roots of *S. flavescens* (1 kg; Tsumura) were extracted with 3 L of acetone at room temperature for 24 h and then filtered. This process was repeated three times. The filtrate was evaporated under reduced pressure to give an acetone extract (14.8 g). The residue was extracted with 3 L of MeOH, and the filtrate was evaporated to give a MeOH extract (91.3 g). Since an active ingredient was included in the acetone extract, the acetone extract was subjected to SiO₂ (AP-300: Toyota Kako Co., Ltd., Aichi, Japan) column purification (CHCl₃/MeOH 20:1 → 10:1 → 0:1) in the stepwise gradient mode and fractions of 100 mL were collected. According to their thin-layer chromatography (TLC, Silica gel 60 F₂₅₄, silica gel RP-18 F_{254S}: Merck KGaA, Darmstadt, Germany) profiles, the resulting fractions were combined into six fractions (frs. 1–6). Fr. 3 was further purified by preparative TLC (CHCl₃/MeOH, 6:1) to obtain an active compound (98 mg).

The structure of the active compound was identified as kurarinone based on comparisons with ¹H and ¹³C-NMR spectroscopic data in the literature [15]. NMR spectra were recorded using a JNM-AL-400 spectrometer (JEOL Ltd., Tokyo, Japan) with tetramethylsilane as the internal standard. Kurarinone: ¹H-NMR (acetone-*d*₆, 400 MHz) δ 7.35 (1H, d, *J* = 8.3 Hz), 6.44 (1H, d, 2.4 Hz), 6.41 (1H, dd, *J* = 8.3, 2.4 Hz), 6.16 (1H, s), 5.58 (1H, dd, *J* = 13.2, 2.9 Hz), 4.94 (1H, br t, *J* = 6.8 Hz), 4.53 (1H, d, *J* = 10.2 Hz), 3.69 (3H, s), 2.82 (1H, dd, *J* = 16.6, 13.2 Hz), 2.65 (1H, m), 2.62 (2H, m), 2.51 (1H, m), 2.01 (2H, m), 1.61 (3H, s), 1.52 (3H, s), 1.43 (3H, s); ¹³C-NMR (acetone-*d*₆, 100 MHz) δ 189.9 (C-4), 163.9 (C-7), 162.7 (C-9), 161.2 (C-5), 159.1 (C-4'), 155.9 (C-6'), 149.2 (C-8a), 131.5 (C-5a), 128.4 (C-2'), 124.5 (C-4a), 118.3 (C-1a), 111.1 (C-9a), 108.5 (C-8), 107.7 (C-3'), 106.0 (C-10), 103.4 (C-5'), 93.4 (C-6), 75.0 (C-2), 55.7 (5-OMe), 47.7 (C-2a), 45.6 (C-3), 31.9 (C-3a), 28.0 (C-1a), 25.8 (C-6a), 19.1 (C-10a), 17.8 (C-7a).

4.9. Chemicals

Tunicamycin (TM) and thapsigargin (TG) were obtained from Fujifilm-Wako (Osaka, Japan). GSK2656157 and ISRIB were obtained from Cayman Chemical (Ann Arbor, MI, USA). All other chemicals were obtained from Sigma.

4.10. Statistical Analysis

The significance of differences between two groups was evaluated using the two-tailed Student's *t*-test. In multi-group analyses, significance was assessed using a one-way ANOVA with the *post hoc* Tukey-Kramer HSD test.

Supplementary Materials: The following are available online at, Figure S1: The acetone extract of *S. flavescens* roots activated the promoter activity of *TRB3*. Figure S2: ¹H-NMR spectrum (400 MHz, acetone-*d*₆) of kurarinone.

Author Contributions: S.N., and Y.I. (Yasumichi Inoue) designed the experiments; S.N., Y.I. (Yuka Itoh), M.T., Y.I. (Yasumichi Inoue), K.N., Y.H., C.M., and K.Y. performed the experiments; Y.I. (Yasumichi Inoue), M.I., H.M., T.M., and H.H. supervised the study; D.M. and N.O. contributed reagents and tools; Y.I. (Yuka Itoh), Y.I. (Yasumichi Inoue), and H.H. wrote the manuscript; All authors discussed the results and commented on the manuscript.

Funding: This work was supported by a Grant-in-Aid for Scientific Research (C) (No. 15K07936, 15K07937, and 18K06660) from the Japan Society for the Promotion of Science (JSPS), a Grant-in-Aid for Young Scientists (No. 18K16081) from the JSPS, and a Grant-in-Aid for Research at Nagoya City University. This work was also supported by the Oriental Medicine Research Foundation.

Acknowledgments: The authors thank the members of the Hayashi laboratory for their helpful discussions. We acknowledge the assistance of the Research Equipment Sharing Center at Nagoya City University. M.T. was the recipient of a scholarship from Kidani Memorial Trust Foundation.

Conflicts of Interest: The authors declare no conflict of interest.

References

1. Pakos-Zebrucka, K.; Koryga, I.; Mnich, K.; Ljubic, M.; Samali, A.; Gorman, A.M. The integrated stress response. *EMBO Rep.* **2016**, *17*, 1374–1395. [[CrossRef](#)] [[PubMed](#)]
2. Denoyelle, C.; Abou-Rjaily, G.; Bezrookove, V.; Verhaegan, M.; Johnson, T.M.; Fullen, D.R.; Pointer, J.N.; Gruber, S.B.; Su, L.D.; Nikiforov, M.A.; et al. Anti-oncogenic role of the endoplasmic reticulum differentially activated by mutations in the MAPK pathway. *Nat. Cell Biol.* **2006**, *8*, 1053–1063. [[CrossRef](#)] [[PubMed](#)]
3. Hart, L.S.; Cunningham, J.T.; Datta, T.; Dey, S.; Trameire, F.; Lehman, S.L.; Qiu, B.; Zhang, H.; Cerniglia, G.; Bi, M.; et al. ER stress-mediated autophagy promotes Myc-dependent transformation and tumor growth. *J. Clin. Investig.* **2012**, *122*, 4621–4634. [[CrossRef](#)] [[PubMed](#)]
4. Harding, H.P.; Zhang, Y.; Zeng, H.; Novoa, I.; Lu, P.D.; Calton, M.; Sadri, N.; Yun, C.; Popko, B.; Paules, R.; et al. An integrative stress response regulates amino acid metabolism and resistance to oxidative stress. *Mol. Cell* **2003**, *11*, 619–633. [[CrossRef](#)]
5. Castilho, B.A.; Shanmugam, R.; Silva, R.C.; Ramesh, R.; Himme, B.M.; Sattlegger, E. Keeping the eIF2 alpha kinase Gcn2 in check. *Biochim. Biophys. Acta* **2014**, *1843*, 1948–1968. [[CrossRef](#)] [[PubMed](#)]
6. Wortel, I.M.N.; van der Meer, L.T.; Kilberg, M.S.; van Leeuwen, F.N. Surviving stress: Modulation of ATF4-mediated stress response in normal and malignant cells. *Trends Endocrinol. Metab.* **2017**, *28*, 794–806. [[CrossRef](#)] [[PubMed](#)]
7. Negelkerke, A.; Bussink, J.; Mujcic, H.; Wouters, B.G.; Lehmann, S.; Sweep, F.C.; Span, P.N. Hypoxia stimulates migration of breast cancer cells via the Perk/atf4/lamp3-arm of the unfolded protein response. *Breast Cancer Res.* **2013**, *15*, R2. [[CrossRef](#)] [[PubMed](#)]
8. Zeng, P.; Sun, S.; Li, R.; Xiao, Z.X.; Chen, H. HER2 upregulates ATF4 to promote cell migration via activation of ZEB1 and downregulation of E-cadherin. *Int. J. Mol. Sci.* **2019**, *20*, 2223. [[CrossRef](#)]
9. Ameri, K.; Harris, A.L. Activating transcription factor 4. *Int. J. Biochem. Cell Biol.* **2008**, *40*, 14–21. [[CrossRef](#)]
10. Carracedo, A.; Lorente, M.; Egia, A.; Blázquez, C.; García, S.; Giroux, V.; Malicet, C.; Villuendas, R.; Gironella, M.; González-Feria, L.; et al. The stress-regulated protein p8 mediates cannabinoid-induced apoptosis of tumor cells. *Cancer Cell* **2006**, *9*, 301–312. [[CrossRef](#)]
11. Qing, G.; Li, B.; Vu, A.; Skuli, N.; Walton, Z.E.; Liu, X.; Mayes, P.A.; Wise, D.R.; Thompson, C.B.; Maris, J.M.; et al. ATF4 regulates MYC-mediated neuroblastoma cell death upon glutamine deprivation. *Cancer Cell* **2012**, *22*, 631–644. [[CrossRef](#)]
12. Ohoka, N.; Yoshii, S.; Hattori, T.; Onozaki, K.; Hayashi, H. TRB3, a novel ER stress-inducible gene, is induced via ATF4-CHOP pathway and is involved in cell death. *EMBO J.* **2005**, *24*, 1243–1255. [[CrossRef](#)]
13. Sakai, S.; Miyajima, C.; Uchida, C.; Itoh, Y.; Hayashi, H.; Inoue, Y. Tribbles-related protein family members as regulators or substrates of the ubiquitin-proteasome system in cancer development. *Curr. Cancer Drug Target* **2016**, *16*, 147–156. [[CrossRef](#)]
14. Jin, H.R.; Zhao, J.; Zhang, Z.; Liao, Y.; Wang, C.Z.; Huang, W.H.; Li, S.P.; He, T.C.; Yuan, C.S.; Du, W. The antitumor natural compound faltarindiol promotes cancer cell death by inducing endoplasmic reticulum stress. *Cell Death Dis.* **2012**, *3*, e376. [[CrossRef](#)]
15. Ryu, S.Y.; Lee, H.S.; Kim, Y.K.; Kim, S.H. Determination of isoprenyl and lavandulyl positions of flavonoids from *Sophora flavescens* by NMR experiment. *Arch. Pharm. Res.* **1997**, *20*, 491–495. [[CrossRef](#)]

16. Axten, J.M.; Romeril, S.P.; Shu, A.; Ralph, J.; Medina, J.R.; Feng, Y.; Li, W.H.; et al. Discovery of GSK2656157: An optimized PERK inhibitor selected for preclinical treatment. *ACS Med. Chem. Lett.* **2013**, *4*, 964–968. [[CrossRef](#)]
17. Sidrauski, C.; Acosta-Alvear, D.; Khoutorsky, A.; Vedantham, P.; Hearn, B.R.; Li, H.; Gamache, K.; Gallagher, C.M.; Ang, K.K.; Wilson, C.; et al. Pharmacological brake-release of mRNA translation enhances cognitive memory. *Elife* **2013**, *2*, e00498. [[CrossRef](#)]
18. Sidrauski, C.; McGeachy, A.M.; Ingolia, N.T.; Walter, P. The small molecule ISRIB reverses the effects of eIF2 α phosphorylation on translation and stress granule assembly. *Elife* **2015**, *4*, e05033. [[CrossRef](#)]
19. Wang, S.; Kaufman, R.J. The impact of the unfolded protein response on human disease. *J. Cell Biol.* **2012**, *197*, 857–867. [[CrossRef](#)]
20. Ron, D.; Harding, H.P. Protein-folding homeostasis in the endoplasmic reticulum and nutritional regulation. *Cold Spring Harb. Perspect. Biol.* **2012**, *4*, a03177. [[CrossRef](#)]
21. Yang, J.; Chen, H.; Wang, Q.; Deng, S.; Huang, M.; Ma, X.; Song, P.; Du, J.; Huang, Y.; Wen, Y.; et al. Inhibitory effect of kurarinone on growth of human non-small cell lung cancer: An experimental study both in vitro and in vivo studies. *Front. Pharmacol.* **2018**, *9*, 252. [[CrossRef](#)]
22. Kang, T.H.; Jeong, S.J.; Ko, W.G.; Kim, N.Y.; Lee, B.H.; Inagaki, M.; Miyamoto, T.; Higuchi, R.; Kim, Y.C. Inhibitory effect of kurarinone on growth of human non-small cell lung cancer: An experimental study both in vitro and in vivo studies. *J. Nat. Prod.* **2000**, *63*, 680–681. [[CrossRef](#)]
23. Koch, A.; Tamez, P.; Pezzuto, J.; Soejarto, D. Evaluation of plants used for antimalarial treatment by the Maasai of Kenya. *J. Ethnopharmacol.* **2005**, *101*, 95–99. [[CrossRef](#)]
24. Inoue, Y.; Kawachi, C.; Ohkubo, T.; Nagasaka, M.; Ito, S.; Fukuura, K.; Itoh, Y.; Ohoka, N.; Morishita, D.; Hayashi, H. The CDK inhibitor p21 is a novel target gene of ATF4 and contributes to cell survival under ER stress. *FEBS Lett.* **2017**, *591*, 3682–3691. [[CrossRef](#)]
25. Ma, T.; Klann, E. PERK: A novel therapeutic target for neurodegenerative diseases? *Alzheimers Res. Ther.* **2014**, *6*, 30. [[CrossRef](#)]
26. Stockwell, S.R.; Platt, G.; Barrie, S.E.; Zoumpoulidou, G.; Te Poele, R.H.; Aherne, G.W.; Wilson, S.C.; Sheldrake, P.; McDonald, E.; Venet, M.; et al. Mechanism-based screen for G1/S checkpoint activators identifies a selective activator of EIF2AK3/PERK signaling. *PLoS ONE* **2012**, *7*, e28568. [[CrossRef](#)]
27. Bruch, J.; Xu, H.; Rösler, T.W.; De Andrade, A.; Kuhn, P.H.; Lichtenthaler, S.F.; Arzberger, T.; Winklhofer, K.F.; Müller, U.; Höglinger, G.U. PERK activation mitigates tau pathology in vitro and in vivo. *EMBO Mol. Med.* **2017**, *9*, 371–384. [[CrossRef](#)]
28. He, X.; Fang, J.; Huang, L.; Wang, J.; Huang, X. *Sophora flavescens* Ait.: Traditional usage, phytochemistry and pharmacology of an important traditional Chinese medicine. *J. Ethnopharmacol.* **2015**, *172*, 10–29. [[CrossRef](#)]
29. Sohn, H.Y.; Son, K.H.; Kwon, C.S.; Kwon, G.S.; Kang, S.S. Antimicrobial and cytotoxic activity of 18 prenylated flavonoids isolated from medicinal plants: *Morus alba* L., *Morus mongolica* Schneider, *Broussonetia papyrifera* (L.) Vent., *Sophora flavescens* Ait. and *Echinosophora koreensis* Nakai. *Phytomedicine* **2004**, *11*, 666–672. [[CrossRef](#)]
30. Jin, J.H.; Kim, J.S.; Kang, S.S.; Son, K.H.; Chang, H.W.; Kim, H.P. Anti-inflammatory and anti-arthritic activity of total flavonoids of the roots of *Sophora flavescens*. *J. Ethnopharmacol.* **2010**, *127*, 589–595. [[CrossRef](#)]
31. Han, J.M.; Jin, Y.Y.; Kim, H.Y.; Park, K.H.; Lee, W.S.; Jeong, T.S. Lavandulyl flavonoids from *Sophora flavescens* suppress lipopolysaccharide-induced activation of nuclear factor- κ B and mitogen-activated protein kinases in RAW264.7 cells. *Biol. Pharm. Bull.* **2010**, *33*, 1019–1023. [[CrossRef](#)]
32. Seo, O.W.; Kim, J.H.; Lee, K.S.; Lee, K.S.; Kim, J.H.; Won, M.H.; Ha, K.S.; Kwon, Y.G.; Kim, Y.M. Kurarinone promotes TRAIL-induced apoptosis by inhibiting NF- κ B-dependent cFLIP expression in HeLa cells. *Exp. Mol. Med.* **2010**, *44*, 653–664. [[CrossRef](#)]
33. Lee, S.; Chae, M.R.; Lee, B.C.; Kim, Y.C.; Choi, J.S.; Lee, S.W.; Cheong, J.H.; Park, C.S. Urinary Bladder-Relaxant Effect of Kurarinone Depending on Potentiation of Large-Conductance Ca²⁺-Activated K⁺ Channels. *Mol. Pharmacol.* **2016**, *90*, 140–150. [[CrossRef](#)]
34. Lee, S.; Choi, J.S.; Park, C.S. Direct activation of the large-conductance calcium-activated potassium channel by flavonoids isolated from *Sophora flavescens*. *Biol. Pharm. Bull.* **2018**, *41*, 1295–1298. [[CrossRef](#)]
35. Zhang, X.; Jiang, P.; Chen, P.; Cheng, N. Metabolism of kurarinone by human liver microsomes and its effect on cytotoxicity. *Pharm. Biol.* **2016**, *54*, 619–627. [[CrossRef](#)]
36. Cubillos-Ruiz, J.R.; Bettigole, S.E.; Glimcher, L.H. Tumorigenic and immunosuppressive effects of endoplasmic reticulum stress in cancer. *Cell* **2017**, *168*, 692–706. [[CrossRef](#)]

37. Wang, Q.; Mora-Jensen, H.; Weniger, M.A.; Perez-Galan, P.; Wolford, C.; Hai, T.; Ron, D.; Chen, W.; Trenkle, W.; Wiestner, A.; et al. ERAD inhibitors integrate ER stress with an epigenetic mechanism to activate BH3-only protein NOXA in cancer cells. *Proc. Natl. Acad. Sci. USA* **2009**, *106*, 2200–2205. [[CrossRef](#)]
38. Kline, C.L.; Van den Heuvel, A.P.; Allen, J.E.; Prabhu, V.V.; Dicker, D.T.; El-Deiry, W.S. ONC201 kills solid tumor cells by triggering an integrated stress response dependent on ATF4 activation by specific eIF2 α kinases. *Sci. Signal.* **2016**, *9*, ra18. [[CrossRef](#)]
39. Arrillaga-Romany, I.; Chi, A.S.; Allen, J.E.; Oster, W.; Wen, P.Y.; Batchelor, T.T. A phase 2 study of the first imipridone ONC201, a selective DRD2 antagonist for oncology, administered every three weeks in recurrent glioblastoma. *Oncotarget* **2017**, *8*, 79298–79304. [[CrossRef](#)]
40. Nagasaka, M.; Hashimoto, R.; Inoue, Y.; Ishiuchi, K.; Matsuno, M.; Itoh, Y.; Tokugawa, M.; Ohoka, N.; Morishita, D.; Mizukami, H.; et al. Anti-tumorigenic activity of chrysin from *Oroxylum indicum* via non-genotoxic p53 activation through the ATM-Chk2 pathway. *Molecules* **2018**, *23*, 1394. [[CrossRef](#)]
41. Kawarada, Y.; Inoue, Y.; Kawasaki, F.; Fukuura, K.; Sato, K.; Tanaka, T.; Itoh, Y.; Hayashi, H. TGF-beta induces p53/Smads complex formation in the PAI-1 promoter to active transcription. *Sci. Rep.* **2016**, *6*, 35483. [[CrossRef](#)]
42. Nagasaka, M.; Tsuzuki, K.; Ozeki, Y.; Tokugawa, M.; Ohoka, N.; Inoue, Y.; Hayashi, H. Lysine-specific demethylase 1 (LSD1/KDM1A) is a novel target gene of c-Myc. *Biol. Pharm. Bull.* **2019**, *42*, 481–488. [[CrossRef](#)]
43. Miyajima, C.; Inoue, Y.; Hayashi, H. Pseudokinase tribbles1 (TRB1) negatively regulates tumor-suppressor activity of p53 through p53 deacetylation. *Biol. Pharm. Bull.* **2015**, *38*, 618–624. [[CrossRef](#)]
44. Hsieh, C.L.; Botta, G.; Gao, S.; Li, T.; Van Allen, E.M.; Treacy, D.J.; Cai, C.; He, H.H.; Sweeney, C.J.; Brown, M.; et al. PLZF, a tumor suppressor genetically lost in metastatic castration-resistant prostate cancer, is a mediator of resistance to androgen deprivation therapy. *Cancer Res.* **2015**, *75*, 1944–1948. [[CrossRef](#)]
45. Yue, X.; Wang, H.; Zhao, F.; Liu, S.; Wu, J.; Ren, W.; Zhu, Y. Hepatitis B virus-induced calreticulin protein is involved in IFN resistance. *J. Immunol.* **2012**, *189*, 279–286. [[CrossRef](#)]
46. Inoue, Y.; Itoh, Y.; Abe, K.; Okamoto, T.; Daitoku, H.; Fukamizu, A.; Onozaki, K.; Hayashi, H. Smad3 is acetylated by p300/CBP to regulate its transactivation activity. *Oncogene* **2007**, *26*, 500–508. [[CrossRef](#)]
47. Miyoshi, N.; Ishii, H.; Mimori, K.; Takatsuno, Y.; Kim, H.; Hirose, H.; Sekimoto, M.; Doki, Y.; Mori, M. Abnormal expression of TRIB3 in colorectal cancer: A novel marker for prognosis. *Br. J. Cancer* **2009**, *101*, 1664–1670. [[CrossRef](#)]
48. Inoue, Y.; Kitagawa, M.; Taya, Y. Phosphorylation of pRB at Ser612 by Chk1/2 leads to a complex between pRB and E2F-1 after DNA damage. *EMBO J.* **2007**, *26*, 2083–2093. [[CrossRef](#)]
49. International Organization for Standardization. *ISO/TR 23022: Traditional Chinese Medicine—Controlled Vocabulary on Japanese Kampo Crude Drugs*; British Standards Institution: London, UK, 2018.

Sample Availability: Samples of the compounds are available from the authors.



© 2019 by the authors. Licensee MDPI, Basel, Switzerland. This article is an open access article distributed under the terms and conditions of the Creative Commons Attribution (CC BY) license (<http://creativecommons.org/licenses/by/4.0/>).